DOE/JPL-954796-79/7
Distribution Category UC-63, List of 9/26/79

(NASA-CR-162904) ANALYSIS AND EVALUATION IN THE PRODUCTION PROCESS AND EQUIPMENT AREA OF THE LOW-COST SOLAR ARRAY PROJECT Quarterly Report, May - Aug. 1979 (Pennsylvania Univ.) 63 p HC A04/MF A01 CSCL 10A G3/44
N80-20814
Unclas
46745

9950-311

Contract JPL-954796
Quarterly Report May to August 1979
(DRD Line Item 6)

August 1979

H. Goldman and M. Wolf

UNIVERSITY of PENNSYLVANIA

The Moore School of Electrical Engineering

PHILADELPHIA, PENNSYLVANIA 19104

The JPL Low-Cost Silicon Solar Array Project is sponsored by the U.S. Department of Energy and forms part of the Solar Photovoltaic Conversion Program to initiate a major effort toward the development of low-cost solar arrays. This work was performed for the Jet Propulsion Laboratory, California Institute of Technology by agreement between NASA and DOE.

DOE/JPL-954796-79/7
Distribution Category UC-63, List of 9/26/79

ANALYSIS AND EVALUATION IN THE PRODUCTION PROCESS

AND EQUIPMENT AREA

of the

LOW-COST SOLAR ARRAY PROJECT

Contract JPL-954796
Quarterly Report May to August 1979
(DRD Line Item 6)

August 1979

H. Goldman and M. Wolf

The JPL Low-Cost Silicon Solar Array Project is sponsored by the U.S. Department of Energy and forms part of the Solar Photovoltaic Conversion Program to initiate a major effort toward the development of low-cost solar arrays. This work was performed for the Jet Propulsion Laboratory, California Institute of Technology by agreement between NASA and DOE.

Abstract

The energy consumed in manufacturing silicon solar cell modules was calculated for the current process, as well as for 1982 and 1986 projected processes. In addition, energy payback times for the above three sequences are shown.

The module manufacturing energy was partitioned two ways. In one way, the silicon reduction, silicon purification, sheet formation, cell fabrication, and encapsulation energies were found. In addition, the facility, equipment, processing material and direct material lost-in-process energies were appropriated in junction formation processes and full module manufacturing sequences.

A brief methodology accounting for the energy of silicon wafers lost-in-processing during cell manufacturing is described.

Table of Contents

LIST OF TABLES

LIST OF TABLES (cont'd)

LIST OF FIGURES

1. Introduction

The manufacturing methods for photovoltaic solar energy utilization systems consist, in complete generality, of a sequence of individual processes. This process sequence has been, for convenience, logically segmented into five major "work areas": Reduction and purification of the semiconductor material, sheet or film generation, device generation, module assembly and encapsulation, and system completion, including installation of the array and the other subsystems. For silicon solar arrays, each work area has been divided into 10 generalizaed "processes" in which certain required modifications of the work-in-process are performed. In general, more than one method is known by which such modifications can be carried out. The various methods for each individual process are identified as process "options". This system of processes and options forms a two-dimensional array, which is here called the "process matrix".

In the search to achieve improved process sequences for producing silicon solar cell modules, numerous options have been proposed and/or developed, and will still be proposed and developed in the future. It is a near necessity to be able to evaluate such proposals for the technical merits relative to other known approaches, for their economic benefits, and for other techno-economic attributes such as energy consumption, generation and disposal of waste by-products, etc. Such evaluations have to be as objective as possible in light of the available information, or the lack thereof, and have to be periodically updated as development progresses and new information becomes available. Since each individual process option has to fit into a process sequence, technical interfaces between consecutive processes must be compatible. This places emphasis on the specifications for the work-in-process entering into and emanating from a particular process option.

The objective of this project is to accumulate the necessary information as input for such evaluations, to develop appropriate methodologies for the performance of such techno-economic analyses, and to perform such evaluations at various levels.

Energy consumption and corresponding payback times were reviewed for the current production process and for processes which may be used on manufacturing lines in 1982 and 1986. For a proper assessment of the payback times, the entire manufacturing process sequence from the mining of the ore, in this case quartzite, and its reduction to Si, up to the completion of the system, fully installed and ready for operation, should be analyzed. So far, we have only accumulated energy data up through module manufacture. Even for this part of the process sequence, we have so far performed only detailed energy analyses for those processes for which we have completed thourough technology and cost studies. These processes include the SiO_2 reduction in the arc furnace, Cz crystal pulling, slicing, junction formation, and the energy content of encapsulation materials. For the remaining parts of the process sequence, we have inserted data from other studies, such as Iles' 1974 compilation of the solar cell plant energy consumption(1) and Bickler's design data for a \$2.00/W(pk)(2) and a \$0.50/W(pk)(3) Strawman process (1975\$).

These energy consumption studies are summarized into two quantities of interest for energy source systems: 1. the total energy consumed in creating the energy source, and 2. the relation of this "invested" energy to the useful energy output of the system which, for solar energy utilization systems, is often called the "payback time". While the former is a reasonably well defined quantity, which depends primarily on the methods used for creating the energy source, the payback time depends also on the use of the system and is thus less uniquely defined.

2. Energy Payback Times

To calculate payback times for photovoltaic systems, the annual energy output of a unit module area must be known. This power output, for photovoltaic systems, is dependent upon the encapsulated cell efficiency, the module packing factor, the solar insolation, the efficiency of the power conditioning and storage subsystems, and the mismatch of the energy availability and demand statistics. This list of dependencies makes it clear that the output of the module will vary according to climate at the locality of installation, and to the individual load to be satisfied. The factors of influence on the useful system output, outside of the cell efficiency, are combined into the "capacity factor". As a reasonably representative, not too optimistic value for this capacity factor, the number 0.11 has been used, in consequence of the results of several system studies.(4) The capacity factor is essentially independent of the solar cell or module manufacturing process. Consequently, the energy payback time is only partly a function of the energy consumption for the solar module fabrication process, since the other system parameters strongly influence its absolute magnitude. In the calculations of energy payback times, encapsulated cell efficiencies η of 11.5% and 15% were employed for 1978 and 1982, respectively, and for 1986, assuming the use of EFG ribbons, of 12%. To obtain the energy payback times, the unit area annual cell output was calculated as $E = \eta \times 8766 \times 0.11 \times H_{pk}$, H_{pk} being the standardized peak solar irradiance, used as 1 kW(pk)/m^2. The factor 0.11 represents the "capacity factor". Thus, annual energy outputs from a square meter of solar cells of 110.9, 144.6, and 115.7 kWh/m^2y are obtained for 1978, 1982, and 1986, respectively.

It is also to be observed that, since the energy recovery from solar cells is in the form of electrical energy, it is appropriate to convert those energy expenditures which occur in the form of heat of combustion, to equivalent electrical energy by applying the average efficiency of 0.30 experienced by the electric utilities in the conversion from heat of combustion of fuels to electric power delivered to the consumer(5).

3. Energy Consumption in Photovoltaic Solar Array Manufacturing Process Sequences

3.1 Data Sources.

The major sources of information for this energy analysis were data accumulated from LSA project reports and industry interviews. The energy consumed through materials, both direct and indirect materials, was obtained by converting the material consumption to energy units through multiplication with the material energy contents shown in Table I. Where specific information to the contrary was not available, the material energy values were assumed to be in the form of thermal energy. The equipment costs, were converted to energy units expressed on the basis of unit cell area of throughput, by assuming a lifetime of seven years, and an energy content of the equipment which corresponds in value to 2% of the equipment cost.(6) This energy cost has then been converted to a thermal energy using an energy price of \$0.003/kWh(th)(7). Finally, the general energy usage for operating the facility was derived from the machine floor area by using the annual SAMICS utility cost of \$3.74/ft^2(8) and assuming that all of this "indirect" energy, since it is used primarily for lighting, air conditioning, and ventilating, in view of the high heat load in the building, is in the form of electricity at a cost of \$0.0319/kWh(8). The conversion factors for the equipment and facility energies thus become 0.9523 kWh(th)/\$y and 1262 kWh/m^{2}y, respectively.

Table I

Energy Contents of Selected Materials

Material	Original Units	Convenient Units (Thermal kWh's)	Reference
1. Acetic acid	3.28 lb of hi-press. steam plus 0.07 kWh(eℓ)/lb	3.18 kWh/g	1
2. Aluminum (Aℓ)	520x10^6 kWh(th)/ton	0.17 kWh/g	2
3. Ammonia gas (NH_3)	8.05x10^3 Btu/lb	0.00534 kWh/g	3
4. Ammonium Hydroxide 30% (NH_4OH)	-	1.32 kWh/ℓ	4
5. Argon gas	1,100 Btu/lb	1.27x10^{-3} kWh/ℓ	5
6. Butyl acetate	4.32 lb of low-press. steam plus 0.082 kWh(eℓ)/lb	3.21 kWh/g	6
7. Copper (Cu)	16.2x10^6 Btu/ton	5.23 kWh/g	7
8. Energy for exhausting waste fumes without scrubbing.	0.46 kW/1000 ft^3/min	2.56x10^{-2} kWh/ 1000 ft^3	8
9. Freon-14 gas (CF_4)	-	2x10^{-3} kWh/ℓ	9
10. Hydrogen gas	43,300 Btu/lb	2.51x10^{-3} kWh/ℓ	5
11. HF (48%)	7,000 Btu/lb	5.22 kWh/ℓ	5
12. Nitrogen (liquid)	1,330 Btu/lb	0.69 KWh/ℓ	5
13. Nitrogen (gas from liquid)	-	1.44x10^{-3} kWh/ℓ	10
14. Nitric Acid (HNO_3, 67%)	14,500 Btu/lb	13.12 kWh/ℓ	5
15. Oxygen gas (O_2)	830 Btu/lb	7.66 kWh/ℓ	5
16. Phosphorus (solid)	23,790 Btu/lb	1.54x10^{-2} kWh/g	5
17. Phosphine gas (PH_3)	-	0.18 kWh/ℓ	11
18. Phosphorous oxychloride ($POC\ell_3$)	-	0.14 kWh/g	12
19. Plating resist	8,000 Btu/lb	5.20 kWh/ℓ	13
20. Silver	1260x10^6 Btu/ton	0.406 kWh/g	8
21. Sodium Hydroxide (NaOH)	by-product	0	5
22. Toluene	0.05 lb of low-press. steam plus 0.025 kWh(eℓ)/lb	0.0349 kWh/mℓ	14
23. Vacuum pump oil	3,000 kWh(th)/ barrel	18.87 kWh/ℓ	15
24. Wax	2,000 kWh/barrel	1.3x10^{-2} kWh/g	16

References for Table V-I

1. Assumed to be the same as that of acetone, which was taken from "Battelle Columbus Laboratories, Draft Target and Support Document for Developing a Maximum Energy Efficient Improvement Target for SIC 28, Federal Energy Administration, Washington, DC (1976)."

2. J.T. Reding and B.P. Shepherd, "Energy Consumption", Report EPA-G50/2-75-032b, US Environmental Protection Agency, Washington, DC (4/75).

3. Federal Energy Administration, "Project Independence Blueprint", Vol. 3, Federal Energy Administration, Washington, DC (1974).

4. Calculated from the energy content for NH_3 and using a density of 0.824 g/mℓ for the NH_4OH solution.

5. Battelle Columbus Laboratories, Draft Target and Support Document for Developing a Maximum Energy Efficient Improvement Target for SIC 28, Federal Energy Administration, Washington, DC (1976).

6. Assumed to be the same as that of butyl alcohol. See Ref. 5.

7. H. W. Lownie, et al (Battell Columbus Laboratories), "Draft Target Report on Development and Establishment of Energy Efficiency Improvement Targets for Primary Metal Industries", Federal Energy Administration, Washington, DC (9/76).

8. M.G. Coleman, et al., Motorola Final Report, DOE/JPL-954847-78/4, 183(11/78).

9. Estimated as approximately 50% more than the average energy content of all gases.

10. Calculated from the energy content for LN_2 assuming 480 ℓ of gas can be obtained form 1ℓ of LN_2.

11. Estimated as twice the energy content for P(s) plus $3/2H_2(g)$.

12. Estimated as twice the energy content of P(s), plus $\frac{1}{2}O_2$ (g), plus $\frac{3}{2}Cl_2(g)$. The energy content of Cl_2 was taken from ref. 5.

13. Assumed to be the same as that of wood rosin , as given in ref. 5.

14. Taken as that of benzene , as given in ref. 5.

15. Taken as approximately twice the energy content of middle oil distillates.

16. From M. Sittig, "Practical Techniques for Saving Energy in the Chemical Petroleum and Metals Industries", Noyes Data Corporation, Park Ridge, NJ (1977), and using a density of 0.97 g/mℓ for the wax.

3.2 Energy Consumption in Si reduction and purification.

This process group starts with the reduction of SiO_2 in an arc furnace. This is a quite efficient and cost-effective process which is not very likely to be replaced by another approach. In contrast, the following step of Si purification is very inefficient and likely to be replaced by one of several alternate methods under development. Furthest advanced among these is the SiH_4 purification process being prepared for pilot line operations by Union Carbide Corp. It can be expected to be a production process by 1986.

a) Theoretical Material Balance for the Arc Furnace Process.

The chemical reaction of this process is:

$$\begin{array}{lccccccc} & SiO_2 & + & 2C & \rightarrow & Si & + & 2\,CO \\ \text{Atomic Weights:} & 28+2(16) & + & 2(12) & \rightarrow & 28 & + & 2(12+16) \\ & 60 & + & 24 & \rightarrow & 28 & + & 56 \\ \text{Masses, normalized to 1 kg Si out:} & 2.14\text{ kg} & + & 0.86\text{ kg} & \rightarrow & 1\text{ kg} & + & 2\text{ kg} \end{array}$$

According to Dow-Corning (9), the industrially experienced and actual conversion efficiency of SiO_2 to Si is 80%.
The required input is thus: 2.68 kg SiO_2 for 1 kg Si out (Dow-Corning shows 2.71 kg SiO_2).
It is assumed that half of the lost SiO_2 input, or 0.27 kg, is used in the reaction:

$$\begin{array}{lccccccc} & SiO_2 & + & C & \rightarrow & SiO & + & CO \\ \text{Atomic Weights:} & 60 & + & 12 & \rightarrow & 44 & + & 28 \\ & 0.27\text{ kg} & + & 0.05\text{ kg} & \rightarrow & 0.2\text{ kg} & + & 0.12\text{ kg} \end{array}$$

where the SiO is lost at the top of the furnace.
Thus, the total theoretical carbon input would be 0.91 kg C per 1 kg MG-Si output.

b) Theoretical Energy Balance.

The energy required from the electric arc for the reduction of SiO_2 to Si would firstly be expected to equal the heat of formation of SiO_2 at the reduction temperature (ΔH^{0}_{f2000}=210kcal/mol), or 8.7 kWh for 1 kg of Si formed. However, the carbon charged into the furnace also participates in the reaction, and, in its oxidation to CO, supplies approximately 25% of the required energy. Thus, the theoretical minimum energy required from the electric arc would be 6.6 kWh/kg Si.

In addition, energy is required to heat the furnace charge to reaction temperature, an energy which is not recovered. Heating the SiO charge (2.7kg) to the reaction temperature will require approximately 1.2 kWh, plus 0.1 kWh heat of fusion, and heating the carbon (0.9 kg) an additional 0.8 kWh, for a total minimum theoretical energy requirement of 10.8 kWh/Si, outside of the heat loss of the furnace.

c) Experienced Material/Energy Balances.

Table II compares the experienced material and energy balances with the theoretical one. Experience data have been taken from ref. 9 which lists "data from a major manufacturer of MG-Si", ref. 10 which cites data from a not widely distributed Battelle report, and ref. 11 which gives data on an experimental arc furnace run at Elkem. Several observations have resulted from the study of these data:

i. The quality of the data does not justify better than 2-digit precision.

ii. Mining and transportation energy expenditures for quartz and coal are quite variable, depending on source, method, location of user, etc., but are in all cases so small as to be negligible. (It is good that the referenced authors, as well as these investigators, have checked the data, so that this statement can be made with confidence.)

Table II

Material/Energy Balance Data for the Arc-Furnace Process (per kg Si out)

	Theoretical				Dow-Corning								Interlake Production Run				Solarex / Battelle Data			
					Industrial Data				Elkem Exper't.											
	kWh (el)	kg	kWh (th)	F.C. kg	kWh (el)	kg	kWh (th)	F.C. kg	kWh (el)	kg	kWh (th)	F.C. kg	kWh (el)	kg	kWh (th)	F.C. kg	kWh (el)	kg	kWh (th)	F.C. kg
Electrical Energy	8.6				13				44.1				13.5				15.4			
Quartzite		2.14	-	-		2.72	-	-		2.43	-	-		2.77	-	-		3.26	-	-
Wood Chips (4.75 kWh/kg) (25% F.C.)						2.77	13.2	0.69		1.46	6.9	0.37		2.48 (40% H_2O)	8.2	0.15 (6%)		1.77	8.4	0.44
Met. Coal (8.9 kWh/kg) (70% F.C.)						0.84	7.5	0.59		0.51	4.5	0.36		1.05	9.5	0.67		0.66	5.9	0.46
Pet. Coke (8.0 kWh/kg) (87.7% F.C.)						0.44	3.5	0.39		0.28	2.2	0.24		0.28	2.4	0.22		0.83	6.6	0.73
Electrode (9.1 kWh/kg) (99% F.C.)						0.1	0.9	0.1		0.50	4.6	0.50		0.09	0.8	0.09		0.17	1.5	0.17
Totals	8.6	-	2.2	0.86	13	-	25	1.8	44.1	-	18	1.5	13.5	-	20.9	1.13	15.4	-	22	1.8

iii. Energy expenditures for plant operation (lighting, ventilation, crane operation, etc.) and energy content of equipment have evidently not yet been analyzed. We added 1 kWh (el) per kg MG-Si produced as an estimate for these energy expenditures (Tables IV A-C Line 1).

iv. The electrical energy consumption in the industrial processes seems only about a factor of 2 higher than theoretically required.

v. The use of "fixed carbon" (F.C.) is also approximately a factor of 2 higher than theoretically required.

vi. The use of thermal energy is an order of magnitude larger than theoretical. The following reasons prevail:

  1. The oxidation of carbon goes only to CO, with only about 1/3 of the heat of combustion of C to CO_2 utilized.
  2. The carbon sources used contain also combustible volatile components of high heat of combustion (hydrocarbons) which are not utilized.

vii. Both ref.'s 9 and 10 add a considerable energy expenditure for the coking process. The petro coke is, however, a byproduct of gasoline refining, obtained by coking the heavy residues from the distillation process. This coking process provides a higher yield of gasoline. It seems, therefore, that the energy expenditure for the coking process should be attributed to the gasoline production and not to the "coke".

viii. For the conversion from heat of combustion to electrical energy, the factor 0.33 has been used, corresponding the average efficiency of electric power generation in thermal plants. In this, the transmission/distribution losses have been omitted since large power users, such as arc furnace operators, are usually located close to generating plants.

ix. The data given in ref. (9) and Table 13 of ref. (11) do not seem to agree with the standard specifications (12) for "low volatile coal" shown in ref. (9).

x. The energy content of "wood chips" used in ref. (9) is approximately a factor of 2 lower than that of ref.'s 10 and 13, with credance given to the latter. The energy content of the volatile component of the woodchips on the unit mass basis, was originally assumed to equal that of metallurgical coal. However, comparing the total heat of combustion for wood thus obtained with that given in standard tables, after adjustment for moisture content, showed that the energy content of the volatiles of wood, as the only unknown, had to be lower by approximately a factor of 2 than that of the volatiles of coal. There probably is better information on this subject available in the literature, but it was not deemed beneficial to the project to expend more effort on this subject, particularly since this energy does not participate in the reaction, but exits via the off-gas. Thus, both input and output of the energy balance are reduced by an equal amount.

xi. Ref. (9) lists the conversion efficiency of SiO_2 to Si as 80%, but ref. (10) uses only 66%. Nevertheless, ref. (10) arrives at approximately the same total energy consumption.

xii. The July 1977 Dow-Corning quarterly report (14) contains very useful detailed data on this subject, which have been augmented by additional information obtained directly from Interlake.(15)

The final energy balance, which was capable of accounting for 90% of the input energy (Table III contains the interesting finding that nearly half of the energy input to the process leaves the furnace as chemical energy in the off-gas. About 60% of this energy is contained in volatile gases, in good part originating from the wood chips. The other 40% is contained in the carbon monoxide which results from the fixed carbon used to reduce the SiO_2. This off-gas is not utilized at present, but is mostly burned off at the top of the furnace. A utilization of this off-gas could reduce the net energy consumption of the process to approximately one half its current value, and such an improvement has been assumed accomplished for the energy balance projections to 1982 and

Table III

Energy Balance
Arcfurnace Reduction of SiO_2 to Si(MG)

Energy Input (per kg Si output)

Material	Mass kg	Component	Mass %	Mass kg	Energy Content Chem kWh	Energy Content Elect'l kWh
Quartzite	2.77	SiO_2	100	2.77	-	-
Woodchips	2.48	H_2O	40	0.98	-	-
		Fixed C	6	0.15	1.4	-
		Volatiles	54	1.34	E 6.8	-
		Ash	0	0.01	-	-
Petro Coke	0.28	H_2O	6	0.01	-	-
		Fixed C	79	0.22	2.0	-
		Volatiles	15	0.04	0.4	-
		Ash	0	0.01	-	-
Met. Coal (Imperial)	0.53	H_2O	4	0.02	-	-
		Fixed C	64	0.34	3.1	-
		Volatiles	30	0.16	1.7	-
		Ash	2	0.01	-	-
(Sewell)	0.52	H_2O	3	0.02	-	-
		Fixed C	63	0.33	3.0	-
		Volatiles	31	0.16	1.7	-
		Ash	3	0.01	-	-
Electrode	0.09	Fixed C	98	0.09	0.8	-
		Ash	2	0	-	-
Totals (Carbon Containing)	3.90	H_2O	26	1.03	-	-
		Fixed C	29	1.13	10.3	-
		Volatiles	44	1.70	10.6	-
		Ash	1	0.04	-	-
Electrical Energy	-	-	-	-	-	13.5

Energy Output (per kg Si output)

Material	Mass kg	Component	Mass %	Mass kg	Energy Content Chem kWh	Energy Content Thermal kWh
Metal at 1500°C	1			1	8.7	0.8
Off-gas at 290°C	5.08	H_2O	20	1.03	-	0.98
		Volatiles	34	1.70	10.6 (like input)	0.66
		CO	16	2.35	6.6	0.18
Fume and Multiclone at 290°C	0.61	Ash	6	0.04	-	0
		SiO	32	0.20	1.1	0.01
		SiO_2	44	0.27	-	0.02
		C	18	0.11	1.0	0.05
Furnace Heat Loss		Radiation		-	-	0.22-0.36
		Conduction/Convection		-	-	0.07
Subtotals					28.0	3.13
Total Output						31.1
Input						34.4
Unaccounted						3.3

E = estimated

beyond.

For the purification of silicon by the standard $SiHCl_3$ process and the generation of the "Polylog", published data (16) and corroboration (17) were used. The energy consumption data computed on this basis are shown in Table IVA, lines 2,3, and 4, for the $SiHCl_3$ generation, the $SiHCl_3$ distillation, and the $SiHCl_3$ reduction to purified silicon, respectively, and correspondingly in Table IVB.

As an alternate purification process, which can be expected to have replaced the $SiHCl_3$ purification process by 1986, the projected energy consumption data for the SiH_4 process under development at Union Carbide Corp. (18) are detailed in lines 2 and 3 of Table IVC.

TABLE IVA

PROCESS ENERGY CONSUMPTION IN THE CURRENT (1978) MANUFACTURING SEQUENCE FOR SILICON WAFERS.

		Yield or Conversion Rate	Direct Material Energy		Indirect Material Energy		Direct Energy		Equipment and Facility Energy		Total Energy Content of Material in Process		Ref.
			Th	El	Th	El	Th	El	Th	El	Th	El	
1.	SiO_2 reduction (kWh/kg)	2.77 kg SiO_2/ kq MG-Si	-	-	20.9	-	-	13.5	- .	1.0	20.9	14.5	(1)
2.	$SiHCl_3$ generation (kWh/kg)	1.67 kg MG-Si/ kg Si in $SiHCl_3$	34.9	24.2	3.6	2.25	-	0.8	-	0.1	38.5	27.4	(2,3)
3.	$SiHCl_3$ distillation (kWh/kg)	1.0 kg $SiHCl_3$/ kg $SiHCl_3$	38.5	27.4	-	-	40.0	-	-	-	78.5	27.4	(2,3)
4.	$SiHCl_3$ reduction to SG-Si (kWh/kg)	2.67 kg Si in $SiHCl_3$/ kg SG-Si	210	73	27	0.3	200	400	-	-	437	473	(2,3)
5.	Cz crystal growth (kWh/kg)	1.13 kg SG-Si/ kg cyl Si	493	535	-	50.6	-	95	-	2	493	682	(4)
6.	Grinding and Slicing (kWh/m^2)	Area conversion 0.552 m^2/kg cyl Si	894	1236	49	-	-	10.2	-	2	945	1253	(4)
											↳	234	
7.	Electrical Energy Equivalent (kWh/m^2)	Conversion 0.3kWh(el) per kWh(th)									Total:	1537	
8.	Energy Content of Material Lost in Process (kWh (el)/m^2)	dto.										1314	

(1) See Table V-2, columns "Interlake Production Run," and p. V-10, item iii, both of this report.

(2) L.P. Hunt, Proc. 12th IEEE Photovoltaic Spec. Conf., IEEE Cat. No. 76CH1142-9 ED, pp. 347-52 (10/76).

(3) C.S. Fang, et al., Lamar Univ. Report ERDA/JPL 954 343-77/3, pp. 15-46 (9/77).

(4) M. Wolf, H. Goldman and A. Lawson, 13th IEEE Photovoltaic Spec. Conference., Cat. No. 76CH 1319-3, pp. 271-80 (6/78), and this report.

TABLE IV B

PROJECTION FOR 1982 OF PROCESS ENERGIES IN THE MANUFACTURING SEQUENCE FOR SILICON WAFERS

		Yield or Conversion Rate	Direct Material Energy		Indirect Material Energy		Direct Energy		Equipment and Facility Energy		Total Energy		Ref.
			Th	El	Th	El	Th	El	Th	El	Th	El	
1.	SiO_2 reduction (kWh/kg)	2.77 kg SiO_2/ kg MG-Si	-	-	10.3	-	-	13.5	-	1.0	10.3	14.5	(1)
2.	$SiHCl_3$ generation (kWh/kg)	1.67 kg MG-Si kg Si in $SiHO_3$	17.2	24.2	3.6	2.25	-	0.8	-	0.1	20.8	27.35	(2,3)
3.	$SiHCl_3$ distillation (kWh/kg)	1.0 kg $SiHCl_3$/ kg $SiHCl_3$	20.8	27.3	-	-	40.8	-	-	-	61.6	27.3	(2,3)
4.	$SiHCl_3$ reduction to SG-Si (kWh/kg)	2.67 kg Si in $SiHCl_3$/ kg SG-Si	164.2	72.8	27.4	0.3	200	400	-	-	391.6	473.1	(2,3)
5.	Cz crystal growth (kWh/kg)	1.13 kg SG-Si/ kg cyl Si	442.5	534.7	-	11	-	52.5	-	1	442.5	599.1	(4)
6.	Grinding and Slicing (kWh/m^2)	Area conversion 0.846 m^2/kg cyl Si	523.0	708.2	21	0.2	-	5.1	-	1	541.9	717.5	(4)
7.	Electrical Energy Equivalent										↳	162.6	
											Total:	880.	
8.	Energy Content of Material Lost in Process											725.0	

1. Same as for 1978 analysis, but off-gases are recycled
2. L.P. Hunt, Proc. 12th IEEE Photovoltaic Spec. Conf., IEEE Cat. No. 76CH1142-9, ED, pp.347-52 (10/76).
3. C.S. Fang, et al., Lamar Univ. Report ERDA/JPL 954343-77/3, pp. 15-46 (9/77).
4. M. Wolf and H. Goldman, University of Pennsylvania. unpublished JPL Quarterly Reports, and ref. (4) of Table IV A

Table 1VC

PROJECTION FOR 1986 OF PROCESS ENERGIES IN THE MANUFACTURING SEQUENCE

FOR SILICON RIBBON (USING THE SILANE PURIFICATION AND THE MOBIL TYCO EFG PPOCESS)

		Yield or Conversion Rate	Direct Material Energy		Indirect Material Energy		Direct Energy		Equipment and Facility Energy		Total Energy		Ref.
			Th	El	Th	El	Th	El	Th	El	Th	El	
1.	SiC_2 reduction (kWh/kg)	2.77 kg SiO_2/ kg MG-Si	-	-	10.3	-	-	13.5	-	1.0	10.3	14.5	(1)
2.	Silane (SiH_4) production (kWh/kg)	90%	11.4	16.1	-	12.45	207.25	10.53	-	-	218.7	39.1	(2,3)
3.	Chemical vapor deposition of silane (kWh/m^2)	Area conversion 2.575 m^2/kg at 90% yield	84.9	15.2	-	-	-	14$^{(e)}$	-	-	84.9	29.2	
4.	Ribbon growth (kWh/m^2)	95%	89.4	30.8	-	-	-	107	-	-	89.4	137.8	(4)
5.	Electrical Energy Equiv. (kWh/m^2)										↳ Total:	26.8 165	
6.	Energy Content of Material Lost in Process kWh(el)/m^2											20.6	

(e) Estimated
1. As in Table 1V B
2. W.C. Breneman, et al., Union Carbide Corp. (Sisterville, West Va.), Report DoE/JPL-954334-78/5 (12/77)
3. C.S. Fang, et al., Lamar University (Beaumont, TX) Report ERDA/JPL 954343 - 78/1, pp. 11-80 (3/78).
4. F.V. Wald, Mobil-Tyco Corporation (Waltham, MA), Contract No. DoE/JPL 954355

3.3 Energy Consumption in Sheet Generation

The current process group for sheet generation contains Czochralski crystal pulling followed by wafer slicing, either by ID diamond blade sawing, multiblade or multiwire slurry sawing.

The Czochralski process can be expected to be improved both with respect to cost and energy consumption. Competing are the heat exchanger method (HEM) of single crystal growth, and semicrystal casting. All of these processes, however, require sawing, with very substantial kerf losses. Consequently, the energy balance of the sawing processes is dominated by the energy content of the silicon material lost in the kerf. The primary possibility for energy savings lies therefore in the replacement of the bulk crystal growing methods, with subsequent sawing, by one of the ribbon growing methods under development. In the projections, improved Czochralski crystal growing and sawing methods are used for 1982, and a ribbon growing method for 1986.

a) Czochralski crystal growth and slicing.

The analysis of the Czochralski crystal pulling process, was based on a review of an earlier analysis(19) and the addition of newer data from Texas Instruments(20) and Dow Corning(21). The projections contain primarily three improvements of energy impact: a reduction of the crucible usage, an increase in the furnace productivity, and additional technology advances which include better furnace design for reduced energy consumption.

The projected crucible usage reduction is based on the assumption that crucibles can be used for the equivalent of 10 individual crystal pulls, either with re-seeding or (quasi-) continuous pulling, rather than the currently practiced usage for one crystal only.

The second projected reduction of energy consumption is connected with a projected furnace productivity increase. Approximately half of this productivity increase is expected to result from an increase in crystal diameter from the presently common, nominally 75 mm (3") diameter to nominally 100 mm (4") by 1982 and to 150 mm (6") by 1986. The other half of the productivity increase, however, is expected to come from a higher linear pull rate, thus more closely approximating the thermodynamically computed theoretical maximum pull rate. This prediction of a linear pull rate increase is more risky as two currently not adequately explored effects are involved. The first concerns crystal perfection which may decrease with increasing pulling speed and may possibly prevent attainment of the expected pull rates. The second unknown is based on an analysis by Rea (22) who found that the radiative energy transfer from the melt surface and the heater environment to the grown crystal prevents any close approach to the limit growth rates computed in the earlier thermodynamic analyses(23). This spurious radiative heat transfer could, in principle, be reduced by introduction of appropriate heat shields. To what degree this can be achieved in practice, without interfering with other aspects of the crystal growing process, needs to be explored.

Some of the possible reduction in energy consumption is not just related to the productivity increase through a reduction of the time for unit mass crystal growth, during which heat losses occur at a constant rate, but is directly connected with the dependence of the heat losses on the system geometry. The estimates are based on the - only conditionally valid - assumption that the heat losses in unit time are directly related to the crystal geometry change, and thus would increase proportionately to the crystal radius. The increased mass pull rate, which results from the radius increase, however, leads to a reduction of the energy losses inversely proportional to the radius. Finally, the required decrease of the linear pull rate results in a reduction of the energy losses inversely proportional to the square root of the crystal radius.

Twice as large a reduction in energy consumption than by the geometry change is, however, expected to result from technology improvements, consisting in the use of better heat shielding and insulation in future furnace designs. Another technology advance has been assumed in the substantial decrease in usage of replacement parts for the crystal pulling furnace, which reflects itself in reduced energy content of the replacement parts used per unit mass of crystal pulled.

Prior to slicing, the ingots are brought to constant diameter in a grinding process, which, by current production experience, costs 8% of the mass of the crystals grown. With the use of larger diameter crystals, projected for 1982, this grinding loss has been assumed to be reduced to 6%.

A similar analysis has been carried out for the slicing process, both as currently practiced and with projected technology improvements. Data on the current production processes include the multi-blade slurry sawing process (24) and the inside diameter diamond blade sawing process (25,26). Also, experimental and projected data on advanced slicing methods were examined for the multi-blade slurry saw (27,28), for the ID diamond blade saw (29), and for the Yasunaga and Crystal Systems multiwire slurry sawing processes. (30,31) The slurry and the blade packs used in the multi-blade process constitute a substantial indirect materials consumption with significant energy content, as do the diamond saw blades in the ID sawing process.

The slicing technology improvements projected for the 1982 production lines as far as they concern the energy balance, are the results of current experimental runs. For the multi-blade saw, the primary advancement will be a 25% blade thickness reduction, in combination with a 37.5% wafer thickness decrease, to 250 μm wafer thickness and 200 μm kerf, while maintaining the present practical wafer yield of 95%. This results in a 50% increase in the mass to area conversion, to 0.9 m^2 per kg silicon crystal. A similar reduction in wafer thickness is anticipated in the ID sawing process, but without reduction of the kerf. The slurry multi-wire saw, which also could be on the 1982 production lines, can yield wafers with similar thickenss and kerf as the multi-blade slurry saw.

For the 1986 projections, energy consumption data given for the EFG ribbon growing process (32), but not yet reviewed by us, were used.

In consequence of the discussed process improvements, the energy content of the wafers or ribbons of silicon is expected to fall from the 1978 value of 1537 kWh(el)/m^2 to 880 kWh(el)/m^2 in 1982 and 165 kWh(el)/m^2 in 1986 (Tables IVA to C).

3.4 Energy Consumption in the Solar Cell and Module Fabrication Process Sequence

The energy analysis of the solar cell fabrication process sequence is, in some respects, simpler than that for the sequence up through sheet generation, and more complicated in others. It is simpler, because one is dealing only with areas of silicon wafers or ribbons, no longer converting from one material form to another, or from mass units to area units. It is more complicated, however, because there exist many more process options and potential sequences.

In any such sequence, the accumulation of yields from the individual process steps is as important for the energy consumption as it is for the costs. In fact, for the entire process from SiO_2 to finished cells, the energy content of the silicon lost in the various conversions and due to yields of the process steps far exceeds the energy going in direct line into the finished product.

Consequently, the total energy expended for producing a unit of work-in-process (or finished product) leaving a given process step n is described by $E_{n-1}/\lambda_n + \Delta E_n$, where E_{n-1} is the total energy expended for producing a unit of work-in-process entering the respective step, ΔE_n is the total energy needed to process a unit of work-in-process through the step, and λ_n is the yield of the process step. The total energy $E_{T,N}$ expended in a process sequence up to step N (inclusive) is then:

$$E_{T,N} = \frac{E_o + \sum_{n=1}^{N} \Delta E_n \prod_{k=1}^{n} \lambda_k}{\prod_{k=1}^{N} \lambda_k} \qquad (1)$$

where E_o is the energy content of a unit of work-in-process or direct material (e.g. wafer or ribbon) entering into step 1 of the sequence. $E_{T,N}$ is, for instance, the energy shown in the right hand columns headed "Total Energy" in Tables IV A to C and VIIIA to C, or "Subtotal" and Total" in Table VI. These total energies cannot be summed, but can be used for entry as E_{n-1} to another step or sub-sequence. Thus, the data in the left-hand columns headed "Direct Material Energy" or "Input Material" in Table VI, and in Tables IVA to C and VIIIA to C, represent the values of E_{n-1}/λ_n.

The total energy "content" of the input work-in-process required to produce a unit of good output from step n is $\frac{E_{n-1}}{\lambda_n}$, so that the energy content $E_{L,n}$ of the material lost in the step n is given by:

$$E_{L,n} = \left(\frac{1}{\lambda_n} - 1 \right) E_{n-1} \qquad (2)$$

This quantity includes the energy content of all material lost in the preceding steps. The energy given by eq. (2) is an important ingredient of the "add-on-energy" $E_{A,n}$ for a unit of good work-in-process leaving process step n:

$$E_{A,n} = E_{L,n} + \Delta E_n; \qquad (3)$$

Data generated by use of eq. (3) are included, e.g., in the right-hand column headed, "Total Add-On Energy" of Table V, while the left-hand column headed "Energy Content of Lost Silicon" includes data obtained by use of eq. (2), with:

$$E_{n-1} = E_{n-2} + E_{A,n-1} \tag{4}$$

Neither the add-on energies, nor the energy values for material lost in a process step, can be summed directly to obtain the total energy expenditures in a process sequence up to step N inclusively, because of the yields of the process steps subsequent to a given step n. Thus, for a unit area of product to leave step N, the total energy content $E_{L,N,n}$ of the material lost in step n is:

$$E_{L,N,n} = \frac{E_{L,n}}{\prod_{k=n+1}^{N} \lambda_k} \tag{5}$$

and the total add-on energy for the sequence from step 1 to step N, inclusive is given by:

$$E_{A,T} = \sum_{n=1}^{N} \frac{E_{L,n} + \Delta E_n}{\prod_{k=n+1}^{N+1} \lambda_k}\ ; \tag{6}$$

with $\lambda_{N+1}=1$.

Eq. (5) has been applied to obtain the "Totals" for the "Energy of Lost Silicon" in Table VII , and an equivalent relationship for the other energy component totals. The farthest right-hand column of Table VII represents data resulting from application of eq. (6) . The energy content of the total material lost is then simply:

$$E_{L,T} = E_{A,T} - \sum_{n=1}^{N} \Delta E_n \quad . \tag{7}$$

The quantities $E_{L,n}$ and $E_{A,n}$, and correspondingly $E_{L,N,n}$ and $E_{A,T}$, include in the energy content that of all material lost in processing the good, remaining work-in-process. They are therefore not suitable for the determination of the total energy content of the material lost in a sequence of process steps, or of the "total net energy content" of the good work-in-process leaving such a sequence. This total net energy content does not include the energy content of the lost material. Thus its computation has to be based on the net energy contents of the input work-in-process, including consideration of the yields of the subsequent process steps. In analogy to eq. (2), the net energy lost in step n for a unit of good work-in-process leaving this step is:

$$E_{L,n,n} = \left(\frac{1}{\lambda_n} - 1\right) E_{n,n-1} \tag{8}$$

where:

$$E_{n,n-1} = E_o + \sum_{k=1}^{n-1} \Delta E_k \tag{9}$$

is the net energy content of the input work-in-process. Similarly, the total net energy lost in step n for a unit of good work-in-process to leave a process sequence after step N is given by:

$$E_{L,n,N,n} = \frac{E_{L,n,n}}{\prod_{k=n+1}^{N} \lambda_k} \tag{10}$$

and the total lost energy in all process steps by:

$$E_{L,n,T} = \sum_{n=1}^{N} \frac{E_{L,n,n}}{\prod_{k=n+1}^{N+1} \lambda_k} ; \qquad (11)$$

with $\lambda_{N+1} = 1$.

Corresponding to eq. (9), the total net energy content of the good work-in-process, or finished product, leaving step N is:

$$E_{n,T} = E_o + \sum_{k=1}^{N} \Delta E_k ; \qquad (12)$$

This total is represented in the farthest right hand column labeled "Total" in Tables IXA to C, while the entries in the columns labeled "Energy content in lost Si" of those tables represent data according to eq. (10) , and the totals of those columns correspond to eq. (11) as well as eq. (7) .

In the solar cell processing sequence, we have accumulated the energy consumption data for the texture etching and the junction formation processes, and we have examined the direct material content of the encapsulation materials. The metallization and antireflection coating processes are presently being analyzed, and their energy data will be presented in a later report. In addition to these detailed analyses, we have accumulated the energy data for the 1982 \$2.00 /W(pk) and the 1986 \$0.50 /W(pk) JPL Strawman process sequences. From our detail analyses for the individual processes and the available data for the remainder of the sequence, such as the Strawman data, we have synthesized overall process sequence energy consumption and payback time data.

a. Energy Consumption of Junction Formation Processes

The energy consumption of the various present and projected junction formation processes was studied in detail in connection with the analysis of their cost-effectiveness. In the evaluations, SAMICS overhead energy standards were used throughout, except for the 1974 and 1977 experience data shown in Table V, lines 1 and 2.

The wafers or ribbons resulting from the Cz slicing (1978 and 1982), or EFG ribbon (1986) processes were tentatively assumed to be subjected to the same texture etching process, with the same yield, independent of the junction formation processes used or the time frame. This unified wafer preparation consists of a 3-step process sub-sequence (33), which includes the application of an etch-stop (wax) to the back surface of the cell, texturing of the front surface by a hot NaOH etch, and removal of the etch-stop (Table VI). The wafers resulting from this process sub-sequence are assumed to form the input material for the various junction formation processes.

The add-on energies for the junction formation processes are summarized in Table V. These processes have been grouped into present (Table V, lines 2-3), near-term (Table

Table V

PROCESS ENERGIES FOR JUNCTION FORMATION PROCESSES (kWh/m^2)

Process	Yield (%)	Energy Content of Lost Silicon		Mat. Energy	Direct Energy	Equip. Energy	Facil. Energy	Total Add-On Energy		Equiv. El.En'y	Payback Time
		(th)	(el)	(th)	(el)	(th)	(el)	(th)	(el)	(el)	(d)
1. Diffusion (Iles, 1974)	NA	NA	NA	NA	30	NA	32	--	62	62	NA
2. Diffusion (Solarex, 1977)	NA	NA	NA	(a)	19.38	(a)	12.21		-	32.00	NA
3. PH$_3$ Diffusion (Spectrolab, 1978)	99.9	0.97	1.28	0.81	2.39	4.48	2.15	6.26	5.82	7.70	25
4. P Ion Implantation (Varian-Extrion, 1978)	99	9.68	12.79	1.75	20.78	33.44	2.74	44.87	36.31	49.77	164
5. POCl$_3$ diffusion (JPL Strawman, 1982)	99.8	1.11	1.46	0.445	1.97	1.3	0.42	2.86	3.85	4.71	13
6. PH$_3$ Diffusion (Motorola, 1986)	99	0.94	1.41	0.098	6.69	0.74	0.39	1.78	8.49	9.04	24
7. 5-step PH and BSF Diffusion Sequence (Motorola, 1986)*	96.8	4.23	6.39	0.23	14.35	3.58	1.05	7.37	21.79	24.00	65
8. PF$_5$ Ion Implantation Lockheed, 1986)	99.2	0.77	1.14	0.30	0.54	4.46	1.65	5.53	3.39	4.99	14
9. 2-Side Ion Implantation w/Annealing (RCA, 1986)	98.4	1.52	2.27	0.92	7.92	10.82	1.75	13.26	11.94	15.91	43
10. High Thruput P Implantation (Spire, 1986)	99.9	0.095	0.14	0.021	2.12	1.42	0.07	1.54	2.33	2.79	8
11. Unanalyzed P Beam Implantation (Motorola, 1986)	99.8	0.19	0.28	0.01	0.62	0.23	0.13	0.43	1.03	1.16	3
12. Ion Implantation PH$_3$ (JPL Strawman, 1986)	99.8	0.18	0.28	0.0	1.07	1.64	0.31	0.82	1.66	2.21	6
13. Activation Annealing (Motorola, 1986)	99.4	0.57	0.85	0.09	3.1	0.34	0.18	1.00	4.13	4.43	12

(a) = included in Facility Energy
NA = not available

*see Table VI for detail

Conversion Factor:
0.3 kWh (el) = 1 kWh (th)

<u>Energies of Starting Material</u>.

	th	el
1978	965	1279
1982	554	733
1986	92.4	142

Table VI

Energy Components of Surface Preparation Processes Preceding Junction Formation (in kWh/m^2)

Process	Yield	Input Material (th)	Input Material (el)	Ind. Mat. (th)	Processing (el)	Equip. (th)	Facility (el)	Subtotal (th)	Subtotal (el)	Total (el)
1978										
1. Solarex 1977 data		NA	NA	(a)	2.83	(a)	5.72	-		
2. Input Work-in-Process: C_z wafers (Table IVA, Line 6)						-		945	1253	
3. Application of etch stop on back	0.99	954.55	1265.36	0.05	0.5	0.65	0.11	955.25	1266.27	
4. Texturing front surface	0.992	962.95	1276.48	-	0.08	0.15	0.068	963.12	1276.62	
5. Removal of etch-stop on back	0.998	965.05	1279.19	0.001	0.11	0.26	0.065	965.31	1279.36	1562
1982										
1. Input Work-in-Process. Cz wafers (Table IVB, Line 6)								541.9	717.5	
2. Application of etch stop on back	0.99	547.37	724.75	0.05	0.5	0.65	0.11	548.07	725.35	
3. Texturing front surface	0.992	552.19	731.21	--	0.08	0.15	0.068	552.64	731.36	
4. Removal of etch-stop on back	0.998	553.75	732.82	0.001	0.11	0.26	0.065	554.01	733.00	899
1986										
1. Input Work-in-Process: EFG Ribbons (Table IVC, Line 6)				-		-	-	89.4	137.8	
2. Application of etch stop on back	0.99	90.30	139.19	0.05	0.5	0.65	0.11	91.0	139.8	
3. Texturing front surface	0.992	91.73	140.73	-	0.08	0.15	0.068	91.88	140.86	
4. Removal of etch-stop on back	0.998	92.07	141.36	0.001	0.11	0.26	0.065	92.34	141.55	169

Data for Application of Etch Stop, Texturizing, and Removal of Etch Stop were derived from Motorola (ref. (36)).

(a) Included in facility energy
(NA) Not Applicable

V , line 4) and long range projected junction formation processes (Table V , lines 5-13). For comparison purposes, the 1974 data (1) for the direct energy consumed in a diffusion process have been included in Table V , line 1. Since the data of this reference include indirect energy consumption only for the entire plant, including wafer generation, cell processing, and environmental testing which is probably more connected with the space power cells produced predominantly in 1974, the indirect energy consumption was, for the purposes of this report, allocated to the various process areas in proportion to their direct energy consumption.

The 1978 Spectrolab phosphine diffusion process (Table V , line 3), for which detailed experience data had been made available(34), shows approximately an order of magnitude lower total equivalent electrical energy consumption than Iles' numbers. This energy consumption is, in many respects, comparable to that for the $POCl_3$ diffusion process contained in the JPL 1982 Strawman process (Table V , line 5)(35). It is noteworthy that the "equipment energy," derived from the equipment price as outlined on p. 6 of this report, is the item of highest energy consumption in the Spectrolab process (Table V , line 3).

Motorola's diffusion process data (36), also for phosphine diffusion, are used as a projection to 1986, with the much lower energy content, per m^2, of the silicon ribbon expected to be used then. This difference expresses itself in the energy consumption for lost silicon. Essentially counterbalancing this change, however, is Motorola's assumption of a lower yield. Another significant difference is in the material energy consumption, which is based on Spectrolab's substantial use of acids for quartzware cleaning, an item which is not included in Motorola's data.

Also included in Table V , line 7, is a 5-step process sub-sequence (Motorola) for the formation of both the pn junction and the BSF layer. This 5-step process includes the phosphine diffusion step just discussed. Its five process steps and their energy consumption are detailed in Table VII.

Besides diffusion, ion implantation is presently used for junction formation. But in its present practice(37), ion implantation is much more energy intensive than the diffusion process (Table V , line 4). The process energy of ion implantation is, however, projected to decrease significantly through improvements in equipment design. These designs stress higher projected throughput rates relative to material usage, and capital equipment and facility requirements. In contrast, for the diffusion process, the add-on energy is not expected to change substantially since significant future increases in furnace efficiency are not anticipated.

It is also necessary to consider associated processes in the sequence, and the yields in such sequences. Thus, the ion implantation process should never be considered without adding the needed annealing step (Table V , line 13). Consequently, the 5-step pn junction and BSF layer diffusion process and the 2-sided ion implantation process with annealing (Table V , lines 2 and 9, respectively)

Table VII

Add-On Process Energies for Motorola's Five-Step Diffusion Process

(in kWh/m^2)

Process	Yield (%)	Energy Content of Lost Si		Mat. Energy	Direct Energy	Equip. Energy	Facility Energy	Total Add-On Energy		Elec. Equiv. of Total Add-On Energy	Cumulative yield $\prod_{k=n+1}^{5} \lambda_k$	Add-On Energy Needed to Produce 1 m^2 of Mat'l. Leaving Step 5
		(th)	(el)	(th)	(el)	(th)	(el)	(th)	(el)	(el)		(el)
1. Spin-on silica on front surface	99%	0.96	1.427	-	0.61	1.01	0.12	1.969	2.157	2.748	0.968	2.838
2. Back p^+ (boron) diffusion w/BCl_3	99%	0.979	1.449	0.087	6.25	0.745	0.39	1.811	8.089	8.632	0.978	8.825
3. Protection of back surface with spin-on silica	99%	0.9972	1.531	-	0.61	1.01	0.12	2.007	2.261	2.863	0.988	2.898
4. Phosphorous (PH_3) diffusion	99%	1.0175	1.554	0.077	6.69	0.74	0.39	1.8345	8.5335	9.184	0.998	9.202
5. Stripping of both surfaces w/4:1 NH_4:HF	99.8	0.2055	0.3255	0.067	0.012	0.011	0.014	0.2835	0.3515	0.437	-	0.437
TOTALS	96.8	4.227	6.388	0.233	14.354	3.580	1.049	8.037	21.79		0.968	24.2

constitute comparable processes. Differing yields, or assumptions of yields, can have significant influence on the energy consumption. Thus, the lower overall yield (96.4%) of the 5-step Motorola sequence compared to that of the competing ion implantation process (98.4%) accounts for nearly 50% of the difference seen in the energy consumption of the 2 processes. This difference is in favor of the ion implantation for this particular example. Because of the importance of high yields for achieving processes with low energy consumption, most of the 1986 solar module fabrication sequence has been projected to be composed of individual processes of very high yields. Modifying the projected Motorola PH_3 diffusion process to be consistent with Spectrolab's experience of 99.9% yield and, in addition, a 17.5% "capacity factor" for the furnace energy consumption, would reduce its payback time from 24 to 9 days, and that of the 5-step sequence to 33 days. This would then be slightly less than the energy payback time of the competing 2-sided ion implantation process with annealing.

The data of Table V are illustrated in Figure 1. It shows the projected ion implantation processes to require less add-on process energies than the projected diffusion processes. However, after adding the process energy for activation annealing to that of the implantation process leads to comparable energy expenditures and payback times for the future ion implantation processes and the diffusion processes.

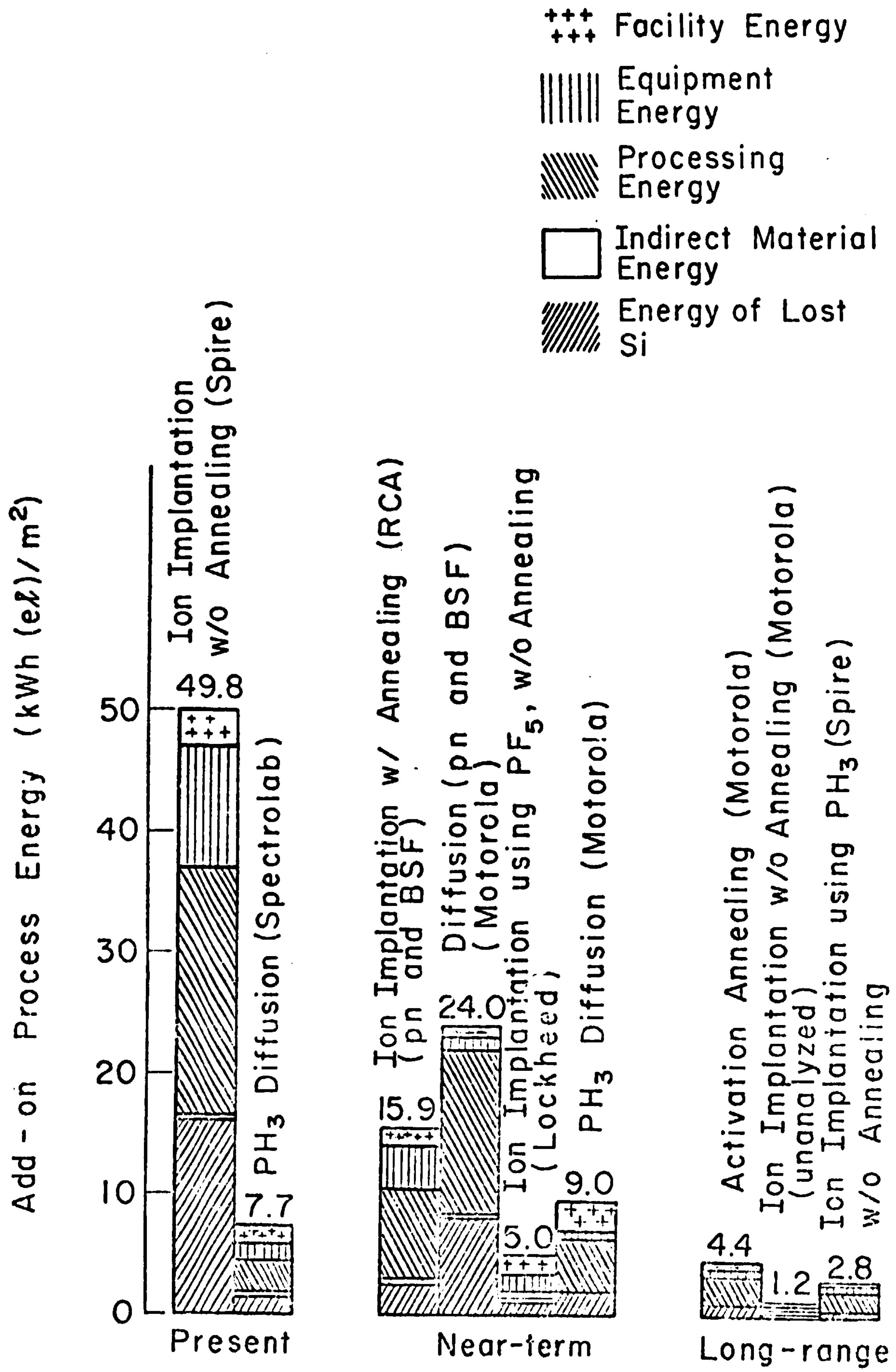

Figure 1: Junction Formation Process Add-On Energies

It may also be noted that the energy payback times for the projected diffusion processes are more "firm" than those for ion implantation, since the latter are based on equipment which has not yet been built. In contrast, the projected diffusion processes represent relatively small extrapolations from current production equipment and practices, primarily modifying throughputs to meet the LSA-JPL output goals.

b. Module assembly (encapsulation)

The major energy contributions in the module assembly step seem to come from the energy content of the encapsulation materials. Consequently, time has not yet been spent on determining the direct energy consumption in the encapsulation process (interconnect attachment, matrix connection, encapsulation material layup, potting material curing, junction box assembly), and the facility energy consumption for the respective part of the plant.

For the 1978 module assembly process, the encapsulation materials chosen were two 3 mm (1/8" thick) glass plates, along with a 1 mm thick layer of potting material. The cell packing density of 80% requires 1.25 m^2 of encapsulation material for each square meter of cell area. Cell yield in this area was tentatively taken as 100%. With a glass energy content of 46.1 kWh/m^2 (38), and a potting material energy content of about 12 kWh/kg, both assumed to be predominantly thermal energy, the energy content of the encapsulation materials .lone is about 130 $kWh(th)/m^2$ of cell area. For the present process, Iles(1) gave no energy consumption data for the encapsulation sequence, but Solarex presented data (39) which are tentatively used in Table VIIIA.

For 1982, an 85% packing factor has been used for the solar cells in the module, reducing the encapsulation area to 1.18 m^2/m^2 of cells, and the energy content of the encapsulation materials to 120 kWh(th)/m^2 of cells. At the same time, the energy consumption data from the JPL \$2/W(pk) Strawman process have been used for the direct energy use and for the facility energy.(35)

For 1986, the packing factor has been assumed to be further improved to 95%, and the back glass layer replaced with a 0.25 mm thick Mylar film, or another material of similar energy content. Use of the improved packing factor alone without back glass replacement, results in an encapsulation material energy content of 107 kWh(th)/m^2 of cells, while use of the Mylar film backing leads to 62 kWh/m^2 of cells. In addition, the relatively small direct and indirect energy consumption data of the 1982 Strawman process for the encapsulation process group have also been used for 1986.

c. Full solar module process sequences.

Using the energy content of the input work-in-process to the solar module fabrication process sequence which was summarized in Tables IVA to C for the current silicon wafers as well as projected wafers (1982) and ribbons (1986), the

Table VIIIA

CURRENT PROCESS ENERGIES IN THE MANUFACTURING SEQUENCE FOR SILICON SOLAR CELL MODULES ALONG WITH THE TOTAL PAYBACK TIME

		Yield or Conversion Rate	Direct Material Energy		Indirect Material Energy		Direct Energy		Equipment and Facility Energy		Total Energy		Ref.
			(th)	(el)	(th)	(el)	(th)	(el)	(th)	(el)	(th)	(el)	
1.	Wafer input	-	-	-	-	-	-		-		945	1253	
2.	Cell processing (kWh/m^2)	80% yield to good cells	1181.3	1566.3	-	76	-	52	8	50	1181.3	1752.3	(1)
3.	Encapsulation (kWh/m^2)	80% packing factor (1.25 m^2 for 1 m^2 of cells)	1181.3	1752.3	130*	-	-	11.1	-	21.0	1311.3	1784.4	(1)
4.	Total equivalent electrical energy consumed (kWh/m^2)	Energy conversion 0.3 kWh(el)/kWh(th)									→	395 Total: 2178	
5.	Payback Time (y)	Recovery rate (110.9 kWh/m^2 y)										19.5	

* Refers to the energy content of the encapsulation material.

(1) J. Lindmayer, et al., Solarex Corp. (Rockville, MD), Report ERDA/JPL 954606-77/1, pp. 48-50 (4/77), and this report.

energy content of the completed modules was estimated or projected, based on available data. It turned out that the differences in these data for current processes are so large that they cannot be significantly improved by introducing the data resulting from our texturizing and junction formation process analysis into these other sequences.

A first analysis of the electrical power requirements of a solar cell production plant had been performed by Iles(1). Iles estimated the contemporary (1974) solar cell fabrication plant energy consumption from the installed equipment power ratings, and extrapolated the plant's productive capacity by assuming that a five times larger solar cell area could be handled annually in the same plant, with approximately the same energy consumption, by going from the then-prevalent 2x2 cm space power cells to 2" diameter cells. Deducting Iles' direct energy consumption values for crystal growing and slicing leaves a direct electrical energy consumption of 120 kWh/m^2 of cell area produced. Allocating the indirect energy consumption in proportion to the direct energy, leads to 125 kWh/m^2 of cell area for the solar cell process plant, These data contain, e.g., a direct energy consumption for diffusion which is an order of magnitude larger than Spectrolab's experience data (see Table V , lines 1 and 2). On the other hand, Iles' data do not contain the energy content of the indirect materials consumed, nor that of the equipment installed (see Table VIIIA).

The Solarex data(39) amount to about half the energy consumption found by Iles, but include the energy contents of the indirect materials consumed and the equipment. Comparing these data with those resulting from the analysis of texturizing and junction formation shows the Solarex energy consumption to be much higher than that given by Motorola for the texturizing process group, and by Spectrolab for diffusion. In contrast, the indirect energy consumption of Solarex (plant lighting etc.) amounts to only 1.7 kWh/m^2 of cells processed and is much lower than any other data given for this item. We consequently increased this consumption to 50kWh/m^2 of cells, or nearly 100% of the direct energy consumption, about in line with the other available data. One reason for this change is also the apparent omission by Solarex of the indirect energy consumption for the common areas, offices, etc.

In the encapsulation area, we used the energy content of the direct materials from section 3.4b of this report, amounting to 130 kWh/m^2 of cells, for 2 sheets of glass and potting material. This number omits the energy content of the interconnectors, a junction box, or a frame possibly applied. Considering these facts, as well as a possibly lower packing factor for Solarex, Solarex's value of 205 kWh/m^2 of cells for this item appears quite compatible. For the direct and the indirect energy consumption in this process step, the Solarex data have been used as the only ones so far available. It may also be noted that 100% cell yield has been assumed for this encapsulation process group, which may be slightly optimistic.

The consequence of these entries is a total energy consumption of 2179 kWh equivalent electrical energy consumed in the production of 1 m^2 of encapsulated cell area. At 80% cell yield from wafers to finished modules, it turns out that 1920 kWh, or 88% of the total module energy content, was already contained in the wafers entering the solar cell processing line. Of the 259 kWh added in the solar cell/module process line, over one quarter is attributable to module assembly and encapsulation.

For the 1982 projections, the summary numbers given for the JPL-Task IV Strawman process (35) have been reviewed. These data include a 93% overall cell processing yield, and an 85% module packing factor. The energy data for the diffusion step in this Strawman process sequence agree quite well with those of the current Spectrolab diffusion process, except for the equipment and facility energy values, which are considerably lower in the Strawman process because of higher assumed throughput rates. This comparison on one significant process step gives a degree of credibility to the remainder of the data. Again, we used our energy content data for the double glass encapsulation. As Table VIIIB shows, the energy content of the completed module has been reduced to about half of that of the 1978 module, but the energy content of the input wafers now constitutes 93% of the module energy content. Also, module assembly and encapsulation now consumes 59% of the cell and module process energy. These shifts are

TABLE V111 B

PROJECTION FOR 1962 of PROCESS ENERGIES IN THE MANUFACTURING SEQUENCE FROM SILICON Cz WAFERS TO SOLAR MODULES

		Yield or Conversion Rate	Direct Material Energy		Indirect Material Energy		Direct Energy		Equip't. Energy	Facility Energy	Total Energy Content		Ref.
			(th)	(el)	(th)	(el)	(th)	(el)	(th)	(el)	(th)	(el)	
1.	Wafer input	--	--	--	--	--	--	--	--	--	541.9	212.5	
2.	Cell processing (kWh/m^2)	93% yield to good cells	582.7	771.5	48.7	-	-	9.0	9.9	4.0	641.3	784.5	(1)
3.	Encapsulation (kWh/m^2)	1.18 m^2 for 1 m^2 of cells	643.6	781.3	121*		-	3.4	2.6	2.9	764.9	790.8	(1)
4.	Total equivalent electrical energy consumed (kWh/m^2)	Energy conversion 0.3 kWh(el)/kWh(th)									→ Total:	229.5 1023	
5.	Payback Time (y)	Recovery rate 144.6kWh/(m^2.y)										7.05	

*Refers to the energy content of the encapsulation material.

1. D. Bickler, Jet Propulsion Laboratory (Pasadena, CA), Interoffice Memo 341-77-D-968 (10/77), and this section.

due primarily to the considerable reduction in energy consumption on the solar cell process line, and are reinforced by the yield improvement on this line from 80% to 90%.

The projections to 1986 were similarly based on the JPL "Candidate Process" data(3) , which lead to a \$0.50/W(pk) encapsulated module price. The input material is assumed to be silane purified, EFG grown ribbon, according to Table IVC. Use of the "Candidate Process" leads to a total energy consumption of 206 kWh/m^2 of equivalent electrical energy (Table VIIIC), of which 173 kWh/m^2, or 84%, is represented in the input ribbon material. Also, 57% of the solar cell and module process energy is added in module assembly, predominantly in the energy content of the encapsulation material.

Tables IXA to C present additional data to augment those of Tables VIIIA to C. They give the mass flow of silicon to the unit of finished encapsulated cell area, the net energy content per unit mass of the work-in-process at the key process stages, as well as the energy content of the silicon lost in the major process groups, and the net process energy of the material appearing in the good finished product, as contributed by these process groups. Again, these data are provided for the contemporary processes and for the projections to 1982 and 1986.

TABLE VIIIC

PROJECTION FOR 1986 OF PROCESS ENERGIES IN THE MANUFACTURING SEQUENCE FROM SILICON EFG RIBBON TO MODULES.

		Yield or Conversion Rate	Direct Material Energy		Indirect Material Energy		Direct Energy		Equipment and Facility Energy		Total Energy		Ref.*
			(th)	(el)	(th)	(el)	(th)	(el)	(th)	(el)	(th)	(el)	
1.	Ribbon input	-	-	-	-	-	-	-	-	-	89.4	137.8	
2.	Cell processing (kWh/m^2)	95%	94.1	145.0	8.1	-	-	7.5	5.65	1.65	107.9	154.1	(1)
3.	Encapsulation	95% packing factor	107.9	154.1	62*	-	-	0.14	0.82	0.1	170,7	154.3	(1)
4.	Total equivalent electrical energy (kWh/m^2)	0.3 kWh (el)/ kWh (th)									↳	51.2 Total: 206	
5.	Payback time (y)	115.7 kWh/m^2.y										1.8	

---

* Refers to the energy content of the encapsulation material.

(1) R.W. Aster, Jet Propulsion Laboratory (Pasadena, CA), LSA Doc. No. 5101-94 (12/78).

Table IXA

ENERGY AND MASS REQUIRED TO PRODUCE 1m^2 of SILICON SOLAR CELLS[(a)]
IN AN ARRAY, AS ESTIMATED FOR 1978 BY THE UNIVERSITY OF PENNSYLVANIA

Process Step	Mass of Si Processed (kg)	Mass of Si lost in Process (kg)	Net energy content of work-in-process (kWh(el)/kg)	Energy content in lost Si (kWh(el))	Energy of Si in finished array for a unit process step (kWh(el))
1. SiO_2 reduction	-	-	-	-	14.5
2. $SiHCl_3$ generation and distillation (1.67 kg/kg)	11.41	4.58	20.8	95.3	11.4
3. $SiHCl_3$ reduction to SG-Si (2.67 kg/kg)	6.83	4.27	37.0	158.1	327.9
4. Cz crystal pulling (1.13 kg/kg)	2.56	0.30	505.4	151.6	103.3
5. Grinding and slicing (0.552 m^2/kg)	2.26	1.39	653.0	907.7	26.9
6. Cell Processing (80% yield)	0.875 (1.25 m^2)	0.175	691.4	121.0	180.4
7. Encapsulation (1.0 m^2 of cells)	0.7 (1.0 m^2)	0			71.1
Totals		10.715		1433.7	735.5
Total Energy Content:				2170 kWh(el)/m^2-Si cells	

(a) Cells are 300 μm thick and the packing factor is 80%.

Table IXB

ENERGY AND MASS REQUIRED TO PRODUCE 1m^2 OF SILICON SOLAR CELLS[(a)]

IN AN ARRAY, AS PROJECTED FOR 1982 BY THE UNIVERSITY OF PENNSYLVANIA

Process Step	Mass of Si Processed (kg)	Mass of Si lost in Process (kg)	Net energy content of work-in-process (kWh(el)/kg)	Energy content in lost Si (kWh(el))	Energy of Si in finished array for a unit process step (kWh(el))
1. SiO_2 reduction	-		-		
		-		-	10.2
2. $SiHCl_3$ generation and distillation (1.67 kg/kg)	6.38		17.6		
		2.55		44.9	9.6
3. $SiHCl_3$ reduction to SG-Si (2.67 kg/kg)	3.83		34.1		
		2.39		81.5	272.9
4. Cz crystal pulling (1.13 kg/kg)	1.44		502.6		
		0.165		83.0	37.0
5. Grinding and slicing (0.846 m^2/kg)	1.27		567.1		
		0.645		365.6	7.3
6. Cell processing (93% yield)	0.626 (1.07 m^2)		579.7		
		0.044		25.4	30.6
7. Encapsulation (1.0 m^2 of cells)	0.583 (1.0 m^2)				43.4
Totals		5.81		600.5	411.0
Total Energy Content:				1012 kWh(el)/m^2-Si cells	

(a) Cells are 250 μm thick and the packing factor is 85%.

Table IXC

ENERGY AND MASS REQUIRED TO PRODUCE 1m^2 OF SILICON SOLAR CELLS[(a)] IN AN ARRAY WITH THE SILANE PURIFICATION AND RTR PROCESSES, AS PROJECTED FOR 1986 BY THE UNIVERSITY OF PENNSYLVANIA

	Process Step	Mass of Si Processed (kg)	Mass of Si lost in Process (kg)	Net energy content of work-in-process (kWh(el)/kg)	Energy content in lost Si (kWh(el))	Energy of Si in finished array for a unit process step (kWh(el)
1.	SiO_2 reduction	-		-		
2.	Silane (SiH_4) Production (90% conversion)	0.48	-	17.59	-	4.1
3.	Chemical Vapor Deposition of silane (2.575 m^2/kg)	0.43	0.05	102.7	0.84	19.8
4.	Ribbon to Ribbon Crystal Re-growth (95% yield)	0.258	0.17	162.8	17.7	14.0
5.	Cell Processing (95% yield)	0.245 (1.05 m^2)	0.013	622.1	2.1	107
6.	Encapsulation	0.233	0.012		7.6	13.2
	Totals					19.1
	Total Energy Content:		0.25		28.3	177.3
					206 kWh(el)/m^2-Si cells	

(a) Cells are 100 μm thick and the packing factor is 95%.

4. Conclusions

The results of the energy consumption analysis are summarized in pictorial form in Fig. 2. This figure clearly demonstrates three points:

a. most of the current high energy content is associated with the losses incurred in material conversion and in process yields.

b. the biggest reductions in the energy consumption will be connected with the introduction of new processes for silicon purification and sheet generation.

c. much of the reduction in cell processing energy comes from higher throughput rates; this effect is already observable now.

The numbers on energy consumption are to be considered as rough approximations, since the data for the current process practice show a large spread, and since the future data represent projections. But in toto, the energy payback times can be expected to decrease rapidly from their recent value near 20 years to below 10 years by 1982 and to less than 2 years by 1986. This last prediction is somewhat obvious since the modules are expected to be close to cost-effective by then as replacement supplies for energy generally available from other sources.

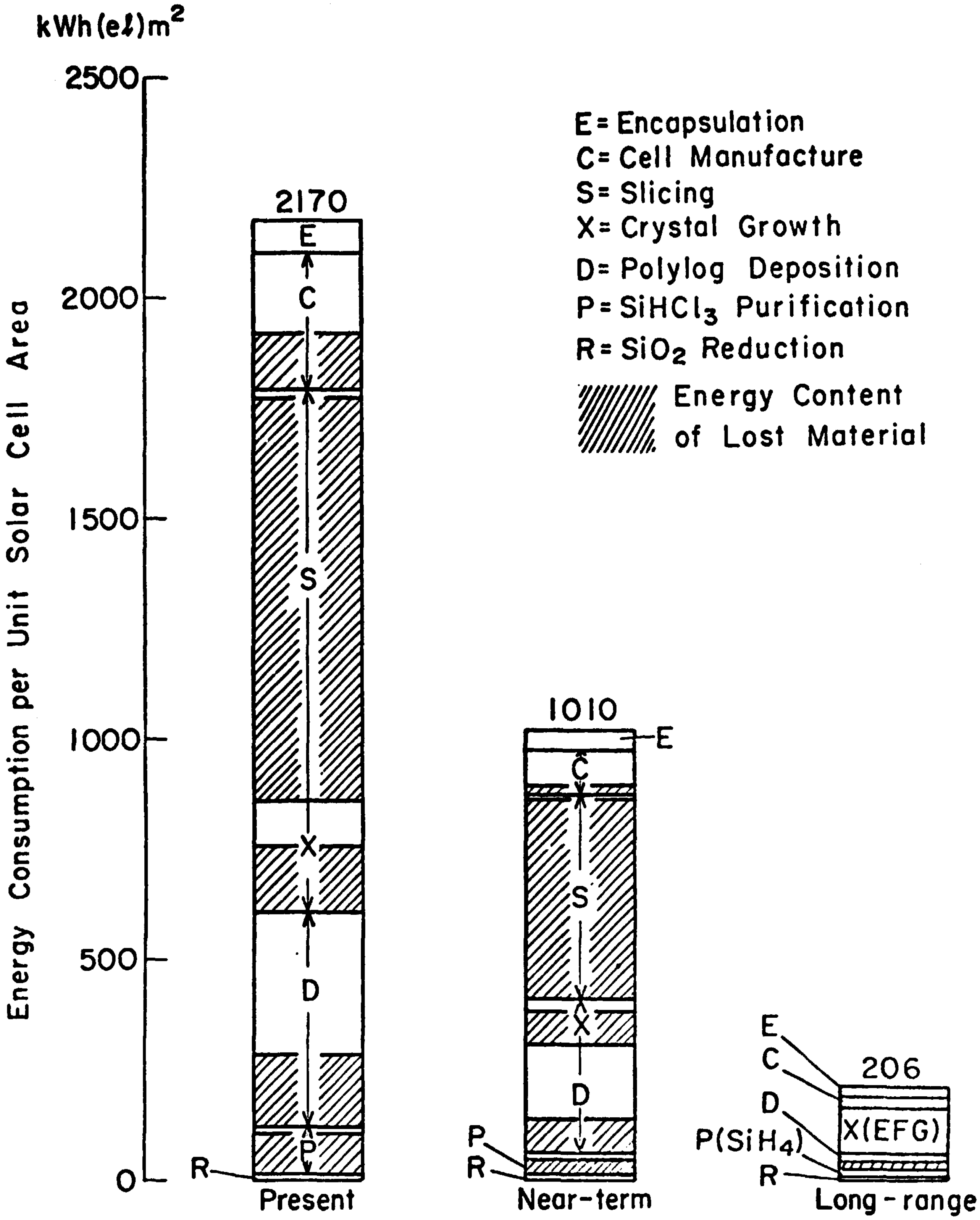

Figure 2: Processing Energy Components For Module Manufacturing

REFERENCES

1. P.A. Iles in "Proceedings of the Material Science Aspects of Thin Film Systems for Solar Energy Conversion," NSF Grant GI-43795, pp. 37-45 (5/74).
2. D.B. Bickler, presented at the 8th JPL-LSA Progress Intergration Meeting (12/77).
3. R.W. Aster, LSA-JPL Report 5101-94 (12/78).
4. M. Wolf, Energy Conversion, <u>16</u>, 79 (1976).
5. "Statistical Yearbook of the Electric Utility Industry for 1970," Edison Electric Institute, New York, NY.
6. National Economic Research Associates, "Energy Consumption and Gross National Product in the United States," NY, NY (1971).
7. US Department of the Interior, "Energy Perspectives 21," US Government Printing Office, Washington, DC (6/79), p. 89.
8. R.W. Aster and R.G. Chamberlain, "Interim Price Estimation Guidelines," JPL-LSA Project Report 5101-33, Pasedena, CA (9/77).
9. L.P. Hunt in "Proc. 12th IEEE Photovoltaic Spec. Conf.," IEEE Cat. No. 76H1142-9 Ed., pp. 78-79 (10/76).
10. J. Lindmayer, et al., Solarex Corp. (Rockville, MD), Report No. ERDA/JPL-954606-77/1, pp. 40-3 (4/77).
11. L.P. Hunt, et al., Dow Corning (Hemlock, Mich.) Report No. ERDA/JPL 954559-76/2, pp. 24-28 (1/77).
12. US Bureau of Mines, "Technology of Lignite Coals," US Bureau of Mines Inform. Circ. 796 (1950).
13. N.A. Lange, ed., Handbook of Chemistry" p. 1505, McGraw-Hill, NY (1961).
14. L.P. Hunt, et al., Dow Corning (Hemlock, Mich) Report ERDA/JPL 954559-77/2, pp. 13-27, (7/77).
15. A. Winkler, Interlake, Inc. Private communication.
16. L.P. Hunt in Proceedings 12th IEEE Photovoltaic Specialists Conference, IEEE Cat. No. 76411429 Ed., pp. 347-52 (10/76).
17. C.S. Fang, et al., Lamar University (Beaumont, TX), Report No. ERDA/JPL 954343-77/3, pp. 15-46 (9/77).

18. W.C. Breman, et al., Union Carbide Corp. (Sisterville, West Virginia), Report DoE/JPL 954334-78/5, pp. (12/77).

19. M. Wolf, et al., University of Pennsylvania (Phila., PA), Final Report ERDA/SE/EG(11-1)-2721/FR/76/1, 187-89 (1/76).

20. S.W. Rea and P.S. Gleim Texas Instruments (Dallas, TX), Final Report ERDA/JPL 954475-77/4, pp. 91-99 (4/77).

21. L.P. Hunt, et al., Dow Corning (Hemlock, Mich.), Report ERDA/JPL-954559-77/2, 32-45 (7/77).

22. S.N. Rea and P.S. Gleim, Texas Instruments (Dallas, TX), Report ERDA/JPL-954475-77/4, 12 (4/77)

23. T.F. Cizek, J. Appl. Phys., 47, p. 440 (1976).

24. R. Oliver, Spectrolab Inc. private communication.

25. H.I. Yoo, Optica [illegible]ing Laboratory Inc., (City of Industry, CA) Report DoE/JPL 954830-77/12, p. 38 (12/77).

26. C. McGinnis, HAMCO (Rochester, NY), private communication.

27. S.N. Rea and P.S. Gleim, Texas Instruments (Dallas, TX), Report ERDA/JPL 954374-77/2, p. 17 (9/77).

28. S.C. Holden and J.R. Fleming, Varian ASsociates (Lexington, MA), Report ERDA/JPL-954374-77/2, p. 22 (7/77).

29. P. Aharonyan, Silicon Technology Corp. (Oakland, NJ), private communications (8/78).

30. J. Lindmayer, et al., Solarex Corp. (Rockville, MD), Report ERDA/JPL 954606-77/2, pp. 11-19 (7-77). Also: C.P. Chen, JPL-LSA Project Report DoE/JPL-1012-75/7 (2/78).

31. F. Schmid and C.P. Khattack, Crystal Systems (Salem MA), Report ERDA/JPL 954373-77/3, pp. 78-79 (10/77).

32. F.V. Wald, Mobil-Tyco Corporation, (Waltham, MA), Contract No. DoE/JPL 954355.

33. M.G. Coleman, et al., Motorola Corporation (Phoenix, AZ), Annual Report DoE/JPL-954847-78/4, (11/78).

34. R. Oliver, Spectrolab Corporation, (Slymar, CA), private communication (4/79).

35. D.B. Bickler, Jet Propulsion Laboratory (Pasadena, CA), JPL-LSA Interoffice Memo 341-77-D-968 (11/10/77).

36. R.A. Pryor, L.A. Grenon, and M.G. Coleman, Motorola Corporation (Phoenix, AZ), Report DoE/JPL-954363-78/8, pp. 133-4, 172 (1/78).

37. J. Munnicci and A. Kirkpatrick, Spire Corporation (Bedford, MA), Report DoE/JPL 954786-78/05, pp. 3, 20-23, (1/78).

38. R.W. Olson, PPG Industries, Inc. (Pittsburgh, PA), private communication (5/78).

39. J. Lindmeyer, et al., Solarex Corporation (Rockville, MD), Report ERDA/JPL-954606-77/1, 48-50 (4/77).

5. NEW TECHNOLOGY STATEMENT

No new technology was developed during this quarter.